SF2A 2014
J. Ballet, F. Bournaud, F. Martins, R. Monier and C. Reylé (eds)

2004 – 2014: TEN YEARS OF RADIATIVE TRANSFER WITH STOKES

F. Marin[1] and R. W. Goosmann[2]

Abstract. Since it became publicly available in 2004, the radiative transfer code STOKES has been used to model the spectroscopic, polarimetric, timing and imaging signatures for different astrophysical scenarios. Ten years later, at the release of a new version of the Monte Carlo code, we make a census of the different scientific cases explored with STOKES and review the main results obtained so far.

Keywords: Polarization, Radiative transfer, Scattering

1 Introduction

STOKES is a Monte Carlo radiative transfer code initially developed by René W. Goosmann for his master thesis that was supervised by C. M. Gaskell. Since 2010, Frédéric Marin contributes significantly to the development of the code and it further benefits from feedback and small extensions implemented by a growing number of users. Originally created to reproduce ultraviolet (UV) and optical polarization measurements in radio-quiet active galactic nuclei (AGN), the code has evolved toward more versatile versions. The latest public version of the code, STOKES 1.2, can be downloaded from the project web page http://www.stokes-program.info/.

STOKES is written in C/C^{++} and simulates the radiative transfer with polarization for multiple scattering, absorption and/or reemission processes in up to 10^4 reprocessing media. The geometry of the emitting source and of the scattering structures can be selected from a list of morphologies (toroidal, spherical, hourglass-shaped, spherical or more complex, segmented structures) and each region can be characterized by its density, temperature and a three-dimensional velocity field. For line emission, Lorentzian flux profiles with user-defined full width at half maximum and intensity are assumed. Thomson, Compton and Mie scattering algorithms, using Mueller matrices and a Stokes vectorial representation, govern the polarization state of the photon from its emission until its eventual escape from the model region. The resulting continuum and line spectra can be evaluated at different inclinations and azimuthal viewing angles since the code is fully three-dimensional. The reader is referred to the user manual of STOKES for further details of the code. Several examples of model calculations can also be found on the web page.

In this conference note, we give a concise overview of major results achieved with STOKES for different astrophysical cases over the last ten years. Note that some of the following results, especially those related to the X-ray domain, are based on more advanced versions than STOKES 1.2 that are not yet public.

2 Applications and results

2.1 Isolated structures

The first public version 1.0 of STOKES was described in Goosmann & Gaskell (2007) and applied to model the effects of different AGN reprocessing morphologies on the UV/optical polarized flux. Dusty tori, polar cones and electron disks were studied for a range of geometrical shapes, opening angles and optical depths. Goosmann & Gaskell (2007) found that the shape of the torus funnel significantly influences the scattering and polarization efficiency, with compact tori (with a steep inner surface) scattering more light along equatorial inclinations than

[1] Astronomical Institute of the Academy of Sciences, Bočni II 1401, 14131 Prague, Czech Republic
[2] Observatoire Astronomique de Strasbourg, Université de Strasbourg, CNRS, UMR 7550, 11 rue de l'Université, 67000 Strasbourg, France

extended tori of the same opening angle. Confined to produce optical* polarization degrees P lower than 20%, circumnuclear structures are less efficient polarizers than polar outflows seen at edge-on (type-2) orientations. While electron-scattering produces wavelength-independent polarization, dusty outflows, representative of the so-called narrow line regions (NLR) in AGN, show reddened spectra for polar inclinations (type-1) and bluer spectra at type-2 viewing angles.

The case of the NLR has been explored in more detail by Goosmann et al. (2007a,b). The authors modeled the polarization induced by Mie reprocessing inside a polar, hourglass-shaped structure filled with two different types of dust. The dust composition and grain size distribution was based on (1) extinction curves observed in our Galaxy (Mathis et al. 1977) and (2) a dust mixture inferred from extinction properties of AGN (Gaskell et al. 2004). When the NLR is filled with dust of the AGN type, weaker polarization spectra and a net decrease of polarization around 4000 Å occur at shorter wavelengths. This is due to a flatter grain size distribution causing a lower scattering efficiency. As a result, AGN dust scatters less flux towards type-2 viewing angles.

2.2 AGN modeling and the polarization dichotomy

2.2.1 The unified model

Once the polarimetric signatures of individual scattering regions explored, the effects of radiative coupling between the inner and outer parts of AGN were included. To do so, three to four reprocessing regions were placed around a central, point source: (1) an equatorial, radiation-supported, fully ionized disk producing most of the polarized flux with a polarization position angle parallel to the symmetry axis of the AGN, (2) an equatorial, obscuring, dusty torus preventing radiation to escape along the midplane, (3) collimated outflows, either filled with electrons (ionized winds) or dust (NLR). Goosmann (2007), Marin & Goosmann (2011), Marin et al. (2012c) and Marin & Goosmann (2012) explored the resulting polarization and stated which constrains can be derived from the observed continuum polarization.

It was found that a flat, equatorial reprocessing region with an optical depth of $1-3$ is required to generate the observed parallel polarization in type-1 AGN, suggesting optically thick accretion flows at the outer edge of type-1 AGN accretion disks. Additionally, a wide torus half-opening angle ($\sim 60°$) enhances the production of parallel polarization, whereas narrow tori and/or a higher optical depth in the polar outflows produce perpendicular polarization when seen at a type-1 viewing angle. At type-2 inclinations, all cases modeled produce strong ($\gg 20\%$) perpendicular polarization. This is not in agreement with previous spectropolarimetric observations of Seyfert-2 galaxies, which report lower ($< 10\%$) polarization percentages. A wide torus/wind half-opening angle helps to mitigate the discrepancy with respect to the observations but the resulting type-2 polarization fraction remains high. Adding the NLR to the three-component model lowers the production of parallel polarization at type-1 viewing angles and helps to decrease the amount of polarization at type-2 viewing angles. A more recent, very careful comparison between the models and the observed polarization has been done in Marin (2014, see also Sect. 2.2.3).

2.2.2 Application to a peculiar case: NGC 1068

The simplest approach of the unified model described in Antonucci (1993) assumes that the accretion disk, the dusty torus and the polar outflows are symmetric with respect to the rotational axis of the disk. In this picture, the alignment of the ejection winds with the circumnuclear, equatorial matter is due to a collimation effect, while a symmetric mass transfer between the inner parts of the torus funnel and the outer edges of the accretion disk would stabilize the two regions along the midplane. However, this picture has been questioned by the mid-infrared interferometric measurements of Raban et al. (2009), who suggest that the polar winds of NGC 1068 (represented as a bi-conical structure) are inclined by 18° with respect to the obscuring torus axis.

To investigate the impact of the non-alignment of the ionized winds on the resulting polarization signature of NGC 1068 and, by extension, on the unified model of AGN, a multi-wavelength study was carried out with STOKES. In the X-ray domain, Goosmann & Matt (2011b,a) explored a variety of AGN inclinations and different hydrogen column densities of the reprocessing material. Under specific conditions, the misalignment of the polar winds with respect to the torus axis can be determined from a rotation of the polarization position angle between the soft and the hard X-ray band. In addition to this, soft X-ray polarimetry can probe the true orientation of the ionization cones. A similar study in the UV/optical waveband by Marin et al. (2012a)

*Goosmann (2009) presents the X-ray counterpart of the optical model and illustrates the performance of an X-ray polarimeter.

successfully reproduces the observed type-1/type-2 polarization dichotomy (i.e. parallel polarization for type-1 AGN and perpendicular polarization at type-2 viewing angles) and shows that the polarization is dominated by scattering in the polar outflows and therefore traces the wind's tilting angle with respect to the torus axis.

2.2.3 Observations versus modeling

Our modeling of NGC 1068 highlights the impact of the system's orientation on the net polarization, in particular for an asymmetric geometry. For a given model, changing the orientation of the observer can lead to significantly different results, especially when the line of sight is close to the horizon of the circumnuclear torus. It is therefore important to examine a given model at all inclinations and to compare the spectropolarimetric results with the observed data. However, this approach was hampered by the lack of a data base combining inclination and polarization information until the recent AGN compendium was gathered by Marin (2014).

The compendium agrees with past empirical results, i.e. type-1 AGN show low polarization degrees ($P < 1\%$) predominantly associated with a parallel polarization position angle while type-2 objects show stronger polarization percentages ($P > 7\%$)[†] with perpendicular polarization angles. The transition between type-1 and type-2 inclination occurs between 45° and 60°, a range likely including AGN classified as borderline objects, where the observer's line of sight crosses the horizon of the equatorial dusty medium. Thanks to this new catalog, the relevance of new AGN models can be investigated more properly.

2.3 The polarization of broad emission lines and off-axis irradiation

The profile and polarization of broad emission lines can put tight constraints on the geometry of the broad line region. The relative offset in blueshift between high and low ionization emission lines could be explained by multiple scattering of the line photons in the accretion flow (Gaskell & Goosmann 2013). The technique of *polarization reverberation mapping* was introduced by Gaskell et al. (2012) as a new way to explore the inner structure of AGN. The cross-correlation between the two light curves of the spectral flux and the polarized flux was established and modeled with STOKES to constrain the distance between the continuum source and the reprocessing mirrors. For this purpose, the code was enabled to take into account timing properties (Goosmann et al. 2008).

Lately, we started to explore the consequences of a new paradigm for the accretion disk emission. Assuming that a significant fraction of the disk's optical/UV luminosity is emitted by temporary off-axis sources (for instance, hot clumps), the characteristic polarization profiles across broad emission lines can be explained in a straightforward manner and do not require any contribution from the equatorial scattering disk nor from rotating winds (Goosmann et al. 2013). Observed polarization variability on time-scales of the BLR light crossing time would strongly support this new interpretation.

2.4 Constraining the morphology of disk-born outflows

Despite a wide panel of observational emission and absorption line features to investigate, the morphology of the inner AGN regions remains debated. Theories interpreting the reprocessing regions of AGN as dynamical structures propose an alternative solution to mostly static media simulated so far (Elvis 2000). In this picture, radiation-driven outflows, potentially responsible for a large fraction of AGN feedback, are launched from the accretion disk over a small range of radii and then bent outward and driven into a radial direction by radiation pressure. Along the equatorial plane, shielded from the full continuum by the highly ionized matter, dust may survive long enough to create a failed dusty wind.

This scenario is alternative to the torus-based unified model and was tested for its polarization properties by Marin & Goosmann (2013b,c,a). A model solely composed of ionized winds is unable to reproduce the expected polarization dichotomy and underestimates the observed optical polarization percentage of both type-1 and type-2 AGN. A dust-filled outflow produces very low, wavelength-dependent polarization degrees, associated with a photon polarization angle perpendicular to the projected symmetry axis of the model; the polarization percentages are ten times lower than what can be produced by a toroidal model, with a maximum polarization degree found at intermediate viewing angles (i.e. when the observers line-of-sight crosses the wind). To

[†]Note that most, if not all, type-2 AGN polarization measurements from the literature are dominated by relatively large, unpolarized starlight fluxes that are insufficiently corrected for (see discussion in Sect. 2.3 of Marin (2014). The revisited polarization of type-2 AGN included in the compendium often have lower limits.

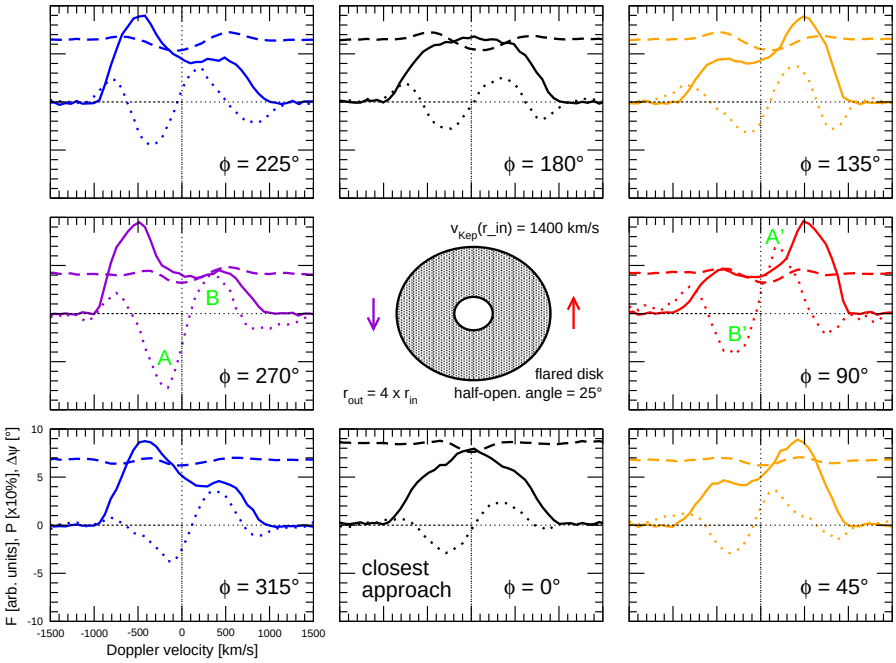

Fig. 1. Modeling the spectropolarimetric appearance of a broad emission line as a function of the azimuthal phase ϕ with an off-axis continuum source. The eight panels show the profile of the line flux, F (solid line), the polarization percentage (dashes), and the variation of the polarization position angle (dots) in Doppler velocity space. Figure taken from Goosmann et al. (2013).

agree with the observations, a two-phase outflow is necessary. It can generate both the observed polarization dichotomy and acceptable levels of polarization degree if the wind has a bending angle of 45° (thus lower than what was predicted by the initial, phenomenological model). The conical shells need to have a half-opening angle comprised between 3° – 10° and the absorbing dust column at the wind base should correspond to an optical depth (integrated over 2000 – 8000 Å) of 1 – 4.

2.5 Probing the physical origin of the asymmetric 6.4 keV iron line

More recent versions of STOKES include radiative processes in the X-ray range. We extended our polarization studies to the 1 – 100 keV band and showed that there is important work to be done for X-ray polarimetry. This new window would be an independent and complementary tool to spectral and timing analyses. We focused on a strongly debated topic of X-ray astrophysics, i.e. the relativistic reflection versus complex absorption scenarios that are proposed to explain the iron line broadening in a number of Seyfert 1 AGN. We managed to derive strong observational predictions for a future spectropolarimetric X-ray mission (Soffitta et al. 2013).

In Marin et al. (2012b), we modeled the polarization signature of MCG-6-30-15 resulting from a partial covering scenario where a clumpy gas distribution is thought to obscure the equatorial plane. We compared the results to a reflection model based on the lamppost geometry and found that the shape of the polarization degree and position angle as a function of photon energy are distinctly different between the reflection and the absorption cases: disk scattering and general relativistic effects produce significantly stronger polarization in the soft energy band than absorption. The spectrum of the polarization angle adds additional constraints: its has a constant value in the absorption case while smooth rotations of the polarization angle with photon energy are detected in the relativistic reflection scenario. We modeled the polarization signature of NGC 1365, a "changing look" AGN where variations of cold absorbers on the line of sight cause extreme and short emission variability. We showed in Marin et al. (2013) that a large, soft X-ray observatory or a medium-sized mission equipped with a hard (6 – 35 keV) polarimeter could break the degeneracy between the two scenarios. We summarized and extended our results in Marin & Tamborra (2013).

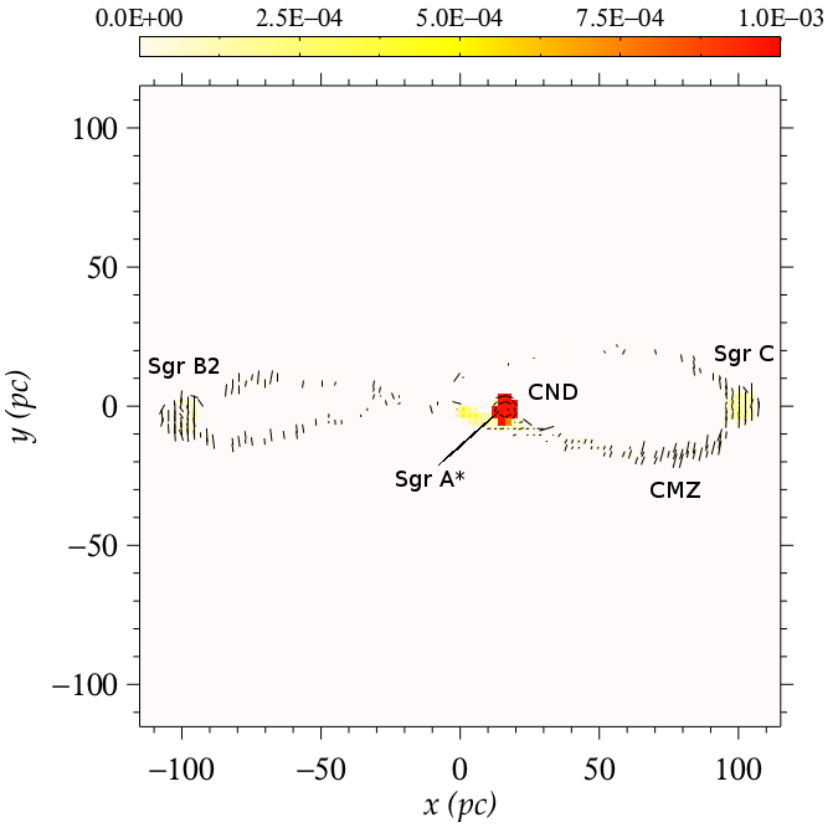

Fig. 2. Integrated 8 – 35 keV model image of the polarized flux, PF/F_*, for the $2^\circ \times 2^\circ$ region around the Galactic Center. PF/F_* is color-coded, with the color scale shown on top of the image (in arbitrary units). The polarization degree and position angle are represented by black bars drawn in the center of each spatial bin. A vertical bar indicates a polarization angle of $\psi = 90^\circ$ and a horizontal bar stands for an angle of $\psi = 0^\circ$. The length of the bar is proportional to P. Figure taken from Marin et al. (2014a)

2.6 X-ray mapping of the Galactic Center

While dedicated to the modeling of AGN, STOKES can be adapted to a variety of other sources, such as the Galactic Center, hosting the closest-to-Earth supermassive black hole. Around the potential well of Sgr A* is a concentration of active star formation sites and gigantic, reprocessing molecular clouds that make the center of the Milky Way an excellent site for X-ray polarization studies. The reprocessing scenario is strongly supported by past X-ray observations of the Eastern massive molecular cloud Sgr B2 that revealed a very steep spectrum with a strong emission line at 6.4 keV related to iron fluorescence. This suggests that part of the diffuse emission of Sgr B2 is due to reprocessing.

The line-of-sight towards Sgr A* being opaque to UV/optical emission, STOKES was applied in the X-ray range to test if a significant X-ray polarization signal could be detected from the Galactic Center. Marin et al. (2014a,b) found that a model where Sgr A* is radiatively coupled to a fragmented circumnuclear disc (CND), an elliptical twisted ring representative of the central molecular zone (CMZ), and the two main, bright molecular clouds Sgr B2 and Sgr C, produces a variety of polarization signatures. Polarization mapping integrated over 8 – 35 keV reveals that Sgr B2 and Sgr C, situated at the two horizontal extensions of the CMZ, present the highest polarization degrees, both associated with a polarization position angle normal to the scattering plane. The CND shows a lower, barely detectable polarization degree and the CMZ polarization is spatially variable. Independently of their spatial location, the two reflection nebulae are found to always produce high polarization degrees ($\gg 10\%$). Finally, it has been shown that a 500 ks observation with a broadband imaging polarimeter on-board of a mid-sized mission could constrain the location and the morphology of the scattering material with respect to the emitting source.

3 Concluding remarks

STOKES is a versatile Monte Carlo code for modeling polarization produced by absorption, reemission and scattering in many astrophysical situations. Its capability to produce UV/optical polarization signatures allows direct comparison with contemporary measurements, but is also a prime tool to evaluate the putative X-ray polarization from different environments. Follow-up investigations in the infrared band are currently under examination. If you have questions about STOKES, contact us by email at admin@stokes-program.info.

The authors thank C. M. Gaskell and F. Tamborra for their involvement in the STOKES code; the former for being behind the firsts lines of the code, the latter for his implication and help in the infrared and X-ray domain. We further acknowledge our colleagues, who keep using STOKES and thank them for their feedback and exciting applications.

References

Antonucci, R. 1993, ARA&A, 31, 473

Elvis, M. 2000, ApJ, 545, 63

Gaskell, C. M. & Goosmann, R. W. 2013, ApJ, 769, 30

Gaskell, C. M., Goosmann, R. W., Antonucci, R. R. J., & Whysong, D. H. 2004, ApJ, 616, 147

Gaskell, C. M., Goosmann, R. W., Merkulova, N. I., Shakhovskoy, N. M., & Shoji, M. 2012, ApJ, 749, 148

Goosmann, R. W. 2007, in Proceedings of RAGtime 8/9: Workshops on Black Holes and Neutron Stars, ed. S. Hledík & Z. Stuchlík, 61–69

Goosmann, R. W. 2009, in SF2A-2009: Proceedings of the Annual meeting of the French Society of Astronomy and Astrophysics, ed. M. Heydari-Malayeri, C. Reyl'E, & R. Samadi, 151

Goosmann, R. W. & Gaskell, C. M. 2007, A&A, 465, 129

Goosmann, R. W., Gaskell, C. M., & Marin, F. 2013, ArXiv e-prints

Goosmann, R. W., Gaskell, C. M., & Shoji, M. 2007a, in IAU Symposium, Vol. 238, IAU Symposium, ed. V. Karas & G. Matt, 375–376

Goosmann, R. W., Gaskell, C. M., & Shoji, M. 2007b, in Astronomical Society of the Pacific Conference Series, Vol. 373, The Central Engine of Active Galactic Nuclei, ed. L. C. Ho & J.-W. Wang, 485

Goosmann, R. W., Gaskell, C. M., & Shoji, M. 2008, in SF2A-2008, ed. C. Charbonnel, F. Combes, & R. Samadi, 231

Goosmann, R. W. & Matt, G. 2011a, in SF2A-2011: Proceedings of the Annual meeting of the French Society of Astronomy and Astrophysics, ed. G. Alecian, K. Belkacem, R. Samadi, & D. Valls-Gabaud, 583–586

Goosmann, R. W. & Matt, G. 2011b, MNRAS, 415, 3119

Marin, F. 2014, MNRAS, 441, 551

Marin, F., Goosmann, R., & Dovčiak, M. 2012a, Journal of Physics Conference Series, 372, 012065

Marin, F. & Goosmann, R. W. 2011, in SF2A-2011: Proceedings of the Annual meeting of the French Society of Astronomy and Astrophysics, ed. G. Alecian, K. Belkacem, R. Samadi, & D. Valls-Gabaud, 597–600

Marin, F. & Goosmann, R. W. 2012, in SF2A-2012: Proceedings of the Annual meeting of the French Society of Astronomy and Astrophysics, ed. S. Boissier, P. de Laverny, N. Nardetto, R. Samadi, D. Valls-Gabaud, & H. Wozniak, 587–590

Marin, F. & Goosmann, R. W. 2013a, MNRAS, 436, 2522

Marin, F. & Goosmann, R. W. 2013b, in SF2A-2013: Proceedings of the Annual meeting of the French Society of Astronomy and Astrophysics, ed. L. Cambresy, F. Martins, E. Nuss, & A. Palacios, 475–478

Marin, F. & Goosmann, R. W. 2013c, in SF2A-2013: Proceedings of the Annual meeting of the French Society of Astronomy and Astrophysics, ed. L. Cambresy, F. Martins, E. Nuss, & A. Palacios, 479–482

Marin, F., Goosmann, R. W., Dovčiak, M., et al. 2012b, MNRAS, 426, L101

Marin, F., Goosmann, R. W., Gaskell, C. M., Porquet, D., & Dovčiak, M. 2012c, A&A, 548, A121

Marin, F., Karas, V., Kunneriath, D., & Muleri, F. 2014a, MNRAS, 441, 3170

Marin, F., Karas, V., Kunneriath, D., Muleri, F., & Soffitta, P. 2014b, ArXiv e-prints

Marin, F., Porquet, D., Goosmann, R. W., et al. 2013, MNRAS, 436, 1615

Marin, F. & Tamborra, F. 2013, ArXiv e-prints

Mathis, J. S., Rumpl, W., & Nordsieck, K. H. 1977, ApJ, 217, 425

Raban, D., Jaffe, W., Röttgering, H., Meisenheimer, K., & Tristram, K. R. W. 2009, MNRAS, 394, 1325

Soffitta, P., Barcons, X., Bellazzini, R., et al. 2013, Experimental Astronomy, 36, 523